Available online at www.sciencedirect.com

ScienceDirect

Procedia Manufacturing 17 (2018) 86–93

Procedia MANUFACTURING

www.elsevier.com/locate/procedia

28th International Conference on Flexible Automation and Intelligent Manufacturing (FAIM2018), June 11-14, 2018, Columbus, OH, USA

Recurrent Neural Network-Based Stencil Cleaning Cycle Predictive Modeling

Haifeng Wang, Tian He, and Sang Won Yoon*

Department of Systems Science and Industrial Engineering
State University of New York at Binghamton
Binghamton, NY 13905, U.S.A

Abstract

This paper presents a real-time predictive approach to improve solder paste stencil printing cycle decision making process in surface mount assembly lines. Stencil cleaning is a critical process that influences the quality and efficiency of printing circuit board. Stencil cleaning operation depends on various process variables, such as printing speed, printing pressure, and aperture shape. The objective of this research is to help efficiently decide stencil printing cleaning cycle by applying data-driven predictive methods. To predict the printed circuit board quality level, a recurrent neural network (RNN) is applied to obtain the printing performance for the different cleaning aging. In the prediction model, not only the previous printing performance statuses are included, but also the printing settings are used to enhance the RNN learning. The model is tested using data collected from an actual solder paste stencil printing line. Based on the predicted printing performance level, the model can help automatically identify the possible cleaning cycle in practice. The results indicate that the proposed model architecture can predictively provide accurate solder paste printing process information to decision makers and increase the quality of the stencil printing process.

Peer-review under responsibility of the scientific committee of the 28th Flexible Automation and Intelligent Manufacturing (FAIM2018) Conference.

Keywords: Recurrent neural network; solder paste stencil printing; predictive modeling

1. Introduction

Solder paste printing (SPP) is one of the critical procedures in applying surface mount technology (SMT) for printed circuit board (PCB) assembly. SPP is the process to selectively deposit solder paste over a PCB surface through a stencil which has etched apertures matching the land patterns on the PCB. For each printing pass, solder is pressed onto the PCB through these apertures using a plastic or metallic squeegee. In practical process, around

* Corresponding author. Tel.: +1-607-777-5935; fax: +1-607-777-4094.
E-mail address: yoons@binghamton.edu

Peer-review under responsibility of the scientific committee of the 28th Flexible Automation and Intelligent Manufacturing (FAIM2018) Conference.
10.1016/j.promfg.2018.10.017

52-71% of SMT defects is related to SPP [5]. Appropriate amount of paste deposition at the right location on PCB is extremely important to reduce defects in PCB assembly line [6]. However, the SPP process is sensitive to many process parameters, such as solder paste type, printing speed, stencil cleaning, etc. In general, these important factors that can affect the SPP quality are classified into three categories: solder paste related, such as solder material, stencil related, such as stencil coating type and preparation, and the printing process parameters, such as printing speed and pressure [6].

Cleaning cycle, which indicates the number of printing intervals/stokes performed before a stencil cleaning, is one of the critical factors that can affect SPP quality [3, 6]. Many studies have analyzed the significance and effects of different cleaning cycle values. However, the method to choose an appropriate cleaning cycle in practical SPP process is rarely studied. The challenge of deciding a correct cleaning cycle derives from two perspectives. Firstly, due to the complexity of the SPP process, many process parameters, such as printing pressure and printing speed, can influence the cleaning cycle. The quantity relation between the cleaning cycle and SPP process characteristics is lack of study, since most of the current studies are to identify significant factors [5]. In addition, the printing parameters are adjusted frequently in many actual processes, which bring the difficulty to choose a generalized optimal cleaning cycle beforehand. To overcome the challenges and improve the SPP process quality, recurrent neural network (RNN) approaches are used to perform stencil cleaning cycle predictive analysis in this research.

The structure of this paper is organized as follows: Section 2 introduces and reviews the characteristics of typical SPP processes. The proposed stencil cleaning cycle predictive control model architecture is illustrated in Section 3. Specifically, the effect of cleaning cycle to SPP quality is also discussed in Section 3. The design of experiments (DOE) dataset and model experimental test results are analyzed and discussed in Section 4. Conclusions and some possible potential extensions of this research are provided in Section 5.

2. Characteristics of solder paste printing process

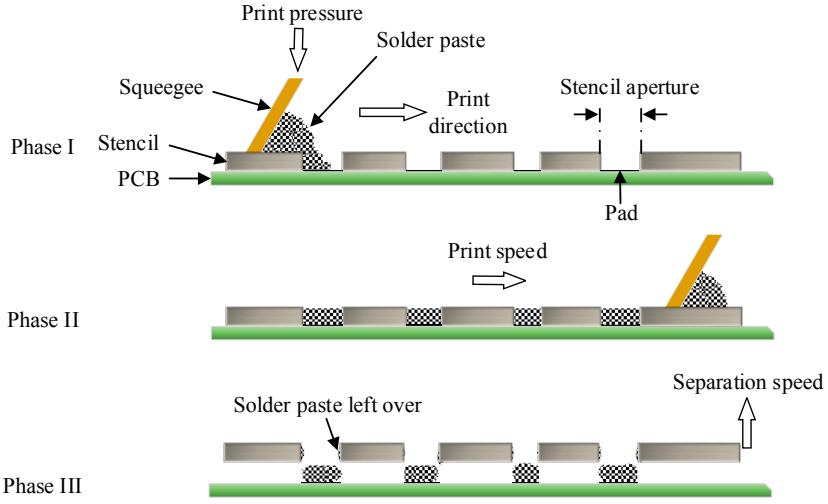

Fig. 1. Solder paste printing process.

The exact procedure and process factors of SPP may vary from printing machine to printing machine. Typically, three phases are included in most of the practical SPP process, as shown in Fig. 1. In Phase I, solder paste is applied on a stencil by squeegee with certain printing pressure. The stencil is designed with etched apertures, which can match the pad location and size pattern on the PCB. Given the printing pressure and direction, solder paste is pressed onto the PCB through apertures by the squeegee with an assigned printing speed in Phase II. Then, Phase III is to lift

up the stencil and convey the PCB out of printer machine. After Phase III, due to some solder paste left over in the stencil aperture, the printing quality of the next printing operation can be influenced. Thus, stencil cleaning becomes a necessary operation. However, frequent stencil cleaning can cost a great amount of production time, while no cleaning may increase the chance of getting defects. Thus, to decide an appropriate cleaning cycle is a critical problem in the SPP process.

Compared to related studies in the literature, there are mainly three contributions from this research: 1) Cleaning cycle was just considered as a factor in DOE studies [3, 6]. The tend of the PCB quality after stencil cleaning is rarely studied in the literature. This research shows the cleaning cycle behavior based on different performance measures in SMT. 2) To achieve the cleaning cycle predictive control, a data sequence analysis has been conducted by using recent advanced sequence analysis models. 3) Typical time series approaches face a big challenge to predict the printing performance because of the frequent change of printing settings, such as printing pressure, printing speed, etc. By developing a RNN model, not only historical process performance information is considered, but also both current and historical printing settings are involved in the prediction process, which can overcome the weakness of time series methods for this problem. Instead of building different models for individual process performance prediction, the proposed RNN model can predict several process performance measures simultaneously.

3. Methodology

SPP process quality is generally presented based on printed solder paste volume. To effectively decide the cleaning cycle, the process quality measures are required to be clearly defined. Also, the influence of the stencil cleaning to the following boards' quality is tested statistically in this section. The details of the RNN model is illustrated at the end of this section.

3.1. SPP process quality trend after cleaning

Solder paste transfer efficiency (SPTE) is a common measure to quantify the quality of transferring paste through stencil aperture to pad. Ideally, the SPTE value should be as close to 100% as possible. Based on SPTE, several SPP quality measures can be defined, such as the average SPTE, denoted as $\bar{v}_j$, average SPTE standard deviation, denoted as $\bar{\sigma}_j$, for the j-th PCB. Based on the SPTE information of each PCB at different cleaning aging i, percentage of pads obtaining SPTE no more than a threshold θ, denoted as D_i^θ, can be calculated to indicate the defect level. Fig. 2 shows the influence of the stencil cleaning to the three printing performance measures, i.e., $\bar{v}_j$, $\bar{\sigma}_j$, and D_i^θ. A stencil cleaning operation is performed just before the PCB marked with circles in Fig. 2. The PCBs marked with star are the outliers detected based on a median absolute deviation (MAD) approach [1]. The details about the data can be found in Section 4.

In terms of the average SPTE $\bar{v}_j$, it is obvious that there is an increase trend, and several printed boards are detected as outliers after stencil cleaning based on MAD detection approach. For average SPTE standard deviation $\bar{\sigma}_j$, PCBs after stencil cleaning tends to reduce the whole board SPTE variation, which indicates the necessary of performing stencil cleaning. For D_i^{60}, where SPTE threshold is selected as 60%, the MAD results show that SPP results after a few boards after stencil cleaning will generate more defects, as shown in Fig. 2(c). The behavior of D_i^{60} indicates that an appropriate cleaning cycle can potentially reduce the whole process defects.

To statistically confirm the existing of trends in the average SPTE ($\bar{v}_j$) and average SPTE standard deviation ($\bar{\sigma}_j$), a Cox-Stuart test, which is a robust trend analysis approach, is used in this research [8]. In the Cox-Stuart test, H_0 assumes no monotonic trend exists in the series, and H_a indicates the existing of monotonic trend in the series. Given a series of data $x_1, x_2, \ldots, x_n$, the Cox-Stuart test includes three steps: 1) Divide the series into two parts: $x_1, \ldots, x_{\frac{n}{2}}$ and $x_{\frac{n}{2}}, \ldots, x_n$; 2) Pair the data with a format of $(x_k, x_{k+\frac{n}{2}})$ for $k = 1, 2, \ldots, \frac{n}{2}$; 3) Calculate statistic value T

$$T = \sum_{\forall k} 1(x_k < x_{k+\frac{n}{2}}), \tag{1}$$

where $1(x_k < x_{k+\frac{n}{2}})$ is an indicator function, which equals 1 if $x_k < x_{k+\frac{n}{2}}$ is true, and 0 if $x_k < x_{k+\frac{n}{2}}$ is false.

Then, if the H_0 is true, T should follow binomial distribution $T \sim B(\frac{n}{2}, \frac{1}{2})$. Based on the Cox-Stuart test results, up to 3 PCBs are detected with significant trend for average SPTE ($\bar{v}_j$), and up to 5 PCBs are detected with significant

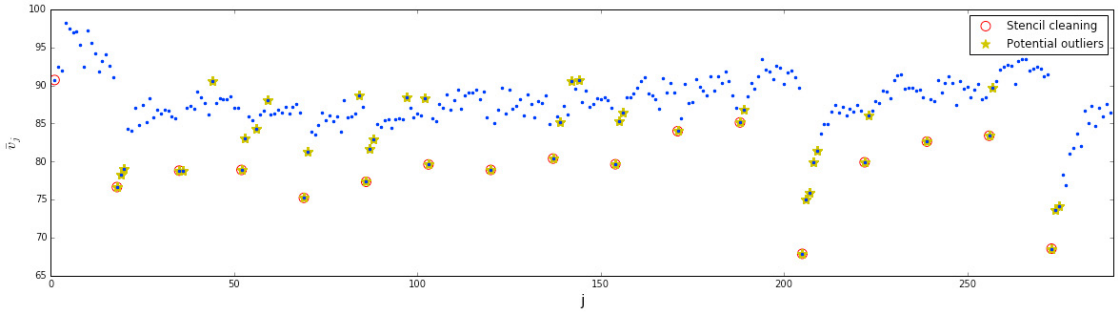

(a) SPTE changing after stencil cleaning.

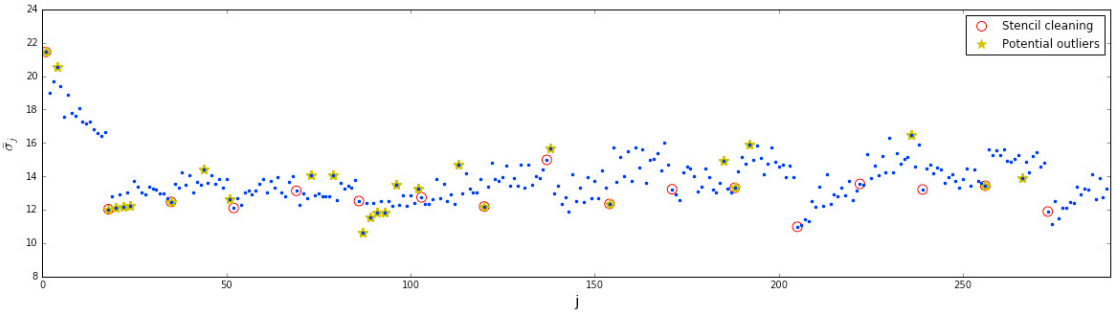

(b) SPTE standard deviation changing after stencil cleaning.

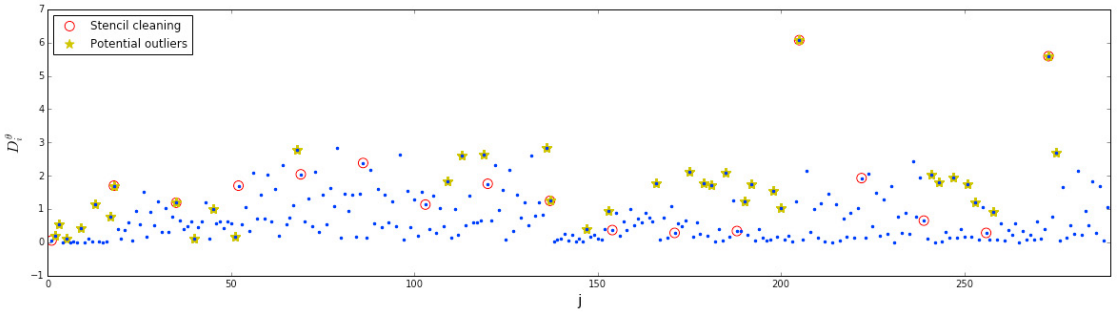

(c) Number of pads obtained low SPTE after stencil cleaning (with $\theta = 60$).

Fig. 2. The influence of stencil cleaning to SPP process quality measures.

trend after stencil cleaning for average SPTE standard deviation ($\bar{\sigma}_j$). Given the existing of the trends in the PCB quality after stencil cleaning, recent advanced sequential analysis models, such as RNN, are used to perform the cleaning cycle predictive control.

3.2. Recurrent neural network-based cleaning cycle prediction

RNNs are typically used for sequence analysis, such as time series data, natural language processing (NLP), etc. Compared to time series models, such as autoregressive integrated moving average (ARIMA), studies have shown that RNNs can obtain satisfactory performances [2]. Long short term memory (LSTM) network is a type of RNN, which has shown a great generalization ability in solving practical problems [7, 4]. LSTM includes memory blocks that can achieve the memory of recent sequence information. Each memory block mainly includes three components: 1) forget gate, which decides what memory information should be removed, 2) input gate, which decides when to update the memory, 3) output gate, which conditionally gives the output based on input and memory. A typical structure of RNN

is illustrated as Equations (2) and (3), where $\boldsymbol{h}_t$ is the state vector, $\boldsymbol{x}_t$ is the input vector, $f^{(\cdot)}(\cdot)$ is the activation function, $\boldsymbol{W}^{(\cdot)}$ and $\boldsymbol{G}^{(\cdot)}$ are weights related to current inputs and previous states, respectively. In this process, history information is used to predict the future process status ($\boldsymbol{y}_t$).

$$\boldsymbol{h}_t = f^h(\boldsymbol{W}^h \boldsymbol{x}_t + \boldsymbol{G}^h \boldsymbol{h}_{t-1}) \tag{2}$$

$$\boldsymbol{y}_t = f^y(\boldsymbol{G}^y \boldsymbol{h}_t) \tag{3}$$

In this research, printing performance (q_i), i.e., $\bar{v}.$, $\bar{\sigma}.$, $D_{\cdot}^{\theta}$, is predicted based on the states of last m PCBs. The history status also includes printer setting information, i.e., printing speed (s_i), printing pressure (p_i), and separation speed (r_i) for the i-th cleaning aging. Fig. 3 shows the process of predicting printing performance, i.e., q_i, at the i-th cleaning aging based on historical and current printing settings and historical printing performance. Each input is transfered to an activation function (f) through a set of weights. And the final prediction is made based on the aggregated information. In particular, the one hidden layer LSTM model can be illustrated in Equations (4)-(9).

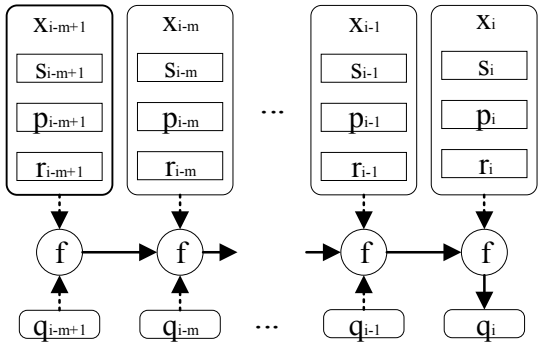

Fig. 3. The SPP performance prediction based on historical process information in the RNN model.

$$\boldsymbol{a}_i = f^a\left[\boldsymbol{W}^a \boldsymbol{x}_i + \sum_{l=i-m+1}^{i-1} (\boldsymbol{P}_l^a \boldsymbol{x}_l + \boldsymbol{E}_l^a \boldsymbol{q}_l) + \boldsymbol{b}^a\right] \tag{4}$$

$$\boldsymbol{c}_i = f\left[\boldsymbol{W}^c \boldsymbol{x}_i + \sum_{l=i-m+1}^{i-1} (\boldsymbol{P}_l^c \boldsymbol{x}_l + \boldsymbol{E}_l^c \boldsymbol{q}_l) + \boldsymbol{b}^c\right] \tag{5}$$

$$\boldsymbol{d}_i = f\left[\boldsymbol{W}^d \boldsymbol{x}_i + \sum_{l=i-m+1}^{i-1} (\boldsymbol{P}_l^d \boldsymbol{x}_l + \boldsymbol{E}_l^d \boldsymbol{q}_l) + \boldsymbol{b}^d\right] \tag{6}$$

$$\boldsymbol{e}_i = f\left[\boldsymbol{W}^e \boldsymbol{x}_i + \sum_{l=i-m+1}^{i-1} (\boldsymbol{P}_l^e \boldsymbol{x}_l + \boldsymbol{E}_l^e \boldsymbol{q}_l) + \boldsymbol{b}^e\right] \tag{7}$$

$$\boldsymbol{z}_i = \boldsymbol{H}_i^c \boldsymbol{a}_i + \boldsymbol{H}_i^d \boldsymbol{z}_{i-1} \tag{8}$$

$$\boldsymbol{y}_i = \boldsymbol{H}_i^e f^a(\boldsymbol{z}_i) \tag{9}$$

where $\boldsymbol{H}_i^c = diag(\boldsymbol{c}_i)$, $\boldsymbol{H}_i^d = diag(\boldsymbol{d}_i)$, $\boldsymbol{H}_i^e = diag(\boldsymbol{e}_i)$, $\boldsymbol{W}^{\cdot}$, $P_l^{\cdot}$, and $E_l^{\cdot}$ are weight vectors related to current printing setting, the l-th cleaning aging printing setting, and the l-th cleaning aging printing performance, respectively. $\boldsymbol{b}^{\cdot}$ are biased variable, and m is backup period.

The objective is to minimize the squared error loss function, as shown in Equation (10).

$$l(q, \hat{q}) = \sum_{i}^{n} (q_i - \hat{q}_i)^2 \tag{10}$$

where q_i is the true printing performance for the i-th cleaning aging, and $\hat{q}_i$ is the predicted printing performance for the i-th cleaning aging, and n is the time period where printing performance is predicted. To enhance the training performance, an adaptive moment estimation (Adam) optimizer, which is an modification version of classical stochastic gradient descent method, is used.

4. Experiment results

4.1. Design of experiment

To collect the practical cleaning cycle related dataset, central composite design (CCD) is used to generate the levels for printing speed, printing pressure, and stencil separation speed. The printing speed levels are 30, 45, and 60 mm/s, the printing pressure levels are 40, 60, and 80 N, the separation speed levels are 1, 3, and 5 mm/s. , as shown in Table 1. For each printing setting combination, stencil cleaning was performed before the first board, and 17 boards were collected.

Table 1. Printing parameter levels from DOE.

No.	Speed (mm/s)	Pressure (N)	Separation speed (mm/s)
1	30	60	3
2	60	60	3
3	45	40	3
4	45	80	3
5	45	60	1
6	45	60	5
7	60	80	5
8	60	80	1
9	60	40	5
10	60	40	1
11	30	80	5
12	30	80	1
13	30	40	5
14	30	40	1
15	45	60	3
16	30	40	3
17	45	60	3

In terms of the LSTM model, all experiments are implemented by TensorFlow r1.5 under the computational specification of 64-bit Windows 10, with Intel i7 processor (4.00 GHz), 16 GB random-access memory (RAM), and NVIDIA GeForce GTX 1080. Three LSTM models are designed for the test, which are denoted as LSTM_H, LSTM_M, and LSTM_S. The related parameter information used in the experimental tested is listed in Table 2.

Table 2. LSTM model parameter information.

Model	Number of layers	Trainable parameters	Training epochs	Batch size	Validation split rate
LSTM_H	3	22,181			
LSTM_M	2	13,861	2,000	10	0.2
LSTM_S	1	5,541			

4.2. Printing performance prediction results

In this experiment, the number of future time period n, whose printing performance will be predicted, is varied from 3 to 5. Two types of prediction performances are measured, which includes mean absolute error (MAE) and

root mean squared error (RMSE) for training (Tr) and testing (Te) processes. In terms of the printing performance variables, i.e., response variables in the prediction process, average SPTE $\bar{v}_{\cdot}$ and average SPTE standard deviation $\bar{\sigma}_{\cdot}$ are considered. For the percentage of pads obtaining SPTE no more than a threshold θ, three thresholds are applied, i.e., 40, 50, and 60. The three LSTM models are tested based on the DOE data collected from the CCD, and results are collected in Tables 3 and 4. All the lowest training and test errors are bold for each row.

In terms of the MAE results based on Table 3, it is obvious that the LSTM_S model outperforms others in predicting most of the printing performances. But, LSTM_H obtains better testing performance in predicting $D_{\cdot}^{40}$, $D_{\cdot}^{50}$, and $D_{\cdot}^{60}$. However, the training error for LSTM_H is not lower than LSTM_S, the cause might due to the lack of enough complexity in estimating the relationships among the historical printing information and current printing performance for LSTM_S. The similar behavior can be found from the RMSE results in Table 4, where LSTM_H outperforms others in terms of testing error when n is 4 and 5. The RMSE results generally validate the finding of MAE results. Considered the prediction period n, all three models tend to get better performance for predicting a shorter future time period. Based on the trend statistical test results shown in Section 2, around 3 to 5 boards are influenced significantly after stencil cleaning, which indicates the prediction of next five boards is pretty enough for the cleaning cycle decision making. The MAE and RMSE results indicates that LSTM_S model should be used to predict $\bar{v}_{\cdot}$ and $\bar{\sigma}_{\cdot}$. Depending on the number of future periods (n) required to predict, different models should be used for $D_{\cdot}^{40}$, $D_{\cdot}^{50}$, and $D_{\cdot}^{60}$. If n is 4 and 5, LSTM_H model should be used, otherwise LSTM_S model should be used.

Table 3. MAE performance results for the three LSTM models on predicting SPP process performance.

n	Printing performance	LSTM_S		LSTM_M		LSTM_H	
		TrMAE	TeMAE	TrMAE	TeMAE	TrMAE	TeMAE
3	$\bar{v}_{\cdot}$	**1.32**	**1.43**	7.53	7.44	7.35	7.50
	$\bar{\sigma}_{\cdot}$	**0.65**	**0.58**	1.24	1.17	1.19	1.19
	$D_{\cdot}^{40}$	**0.07**	**0.06**	**0.07**	0.07	**0.07**	0.08
	$D_{\cdot}^{50}$	0.55	**0.53**	**0.54**	**0.53**	0.56	0.54
	$D_{\cdot}^{60}$	**0.57**	**0.56**	0.70	0.61	0.65	0.72
4	$\bar{v}_{\cdot}$	**1.43**	**1.43**	6.58	6.80	6.69	6.75
	$\bar{\sigma}_{\cdot}$	**0.84**	**0.79**	1.21	1.28	1.23	1.24
	$D_{\cdot}^{40}$	**0.06**	0.08	0.07	0.08	**0.06**	**0.07**
	$D_{\cdot}^{50}$	**0.52**	0.59	0.54	0.58	0.55	**0.54**
	$D_{\cdot}^{60}$	**0.60**	0.66	0.63	0.70	0.67	**0.58**
5	$\bar{v}_{\cdot}$	**4.67**	**4.80**	6.02	6.00	6.08	6.30
	$\bar{\sigma}_{\cdot}$	**1.00**	**1.04**	1.15	1.44	1.29	1.09
	$D_{\cdot}^{40}$	**0.07**	**0.07**	**0.07**	0.08	**0.07**	**0.07**
	$D_{\cdot}^{50}$	0.57	0.60	**0.55**	**0.55**	0.56	**0.55**
	$D_{\cdot}^{60}$	**0.61**	0.66	0.64	0.62	0.66	**0.54**

Table 4. RMSE performance results for the three LSTM models on predicting SPP process performance.

n	Printing performance	LSTM_S		LSTM_M		LSTM_H	
		TrRMSE	TeRMSE	TrRMSE	TeRMSE	TrRMSE	TeRMSE
3	$\bar{v}_{\cdot}$	**1.61**	**1.76**	8.75	8.61	8.61	8.80
	$\bar{\sigma}_{\cdot}$	**0.84**	**0.75**	1.62	1.42	1.53	1.65
	$D_{\cdot}^{40}$	**0.11**	**0.09**	**0.11**	0.11	**0.11**	0.11
	$D_{\cdot}^{50}$	**0.67**	**0.64**	0.68	0.67	0.68	0.67
	$D_{\cdot}^{60}$	**0.75**	**0.71**	0.90	0.76	0.84	1.01
4	$\bar{v}_{\cdot}$	**1.79**	**1.86**	8.35	8.68	8.42	8.47
	$\bar{\sigma}_{\cdot}$	**1.07**	**1.03**	1.54	1.64	1.57	1.56
	$D_{\cdot}^{40}$	**0.10**	**0.11**	**0.10**	0.13	**0.10**	0.13
	$D_{\cdot}^{50}$	**0.66**	0.72	0.68	**0.71**	0.68	**0.71**
	$D_{\cdot}^{60}$	**0.76**	0.78	0.81	0.87	0.85	**0.73**
5	$\bar{v}_{\cdot}$	**6.27**	**6.01**	8.11	8.30	8.19	8.04
	$\bar{\sigma}_{\cdot}$	**1.33**	1.28	1.47	1.83	1.64	**1.26**
	$D_{\cdot}^{40}$	0.11	**0.10**	**0.10**	0.12	0.11	**0.10**
	$D_{\cdot}^{50}$	**0.69**	0.70	**0.69**	0.72	**0.69**	**0.69**
	$D_{\cdot}^{60}$	**0.78**	0.79	0.79	0.76	0.82	**0.63**

The actual defect level and predicted defect level are illustrated in Fig. 4. The prediction configuration is based on LSTM_H and $n = 4$. It is obvious that the LSTM model can correctly capture the process defect variation and achieve a high prediction consistency with the actual process.

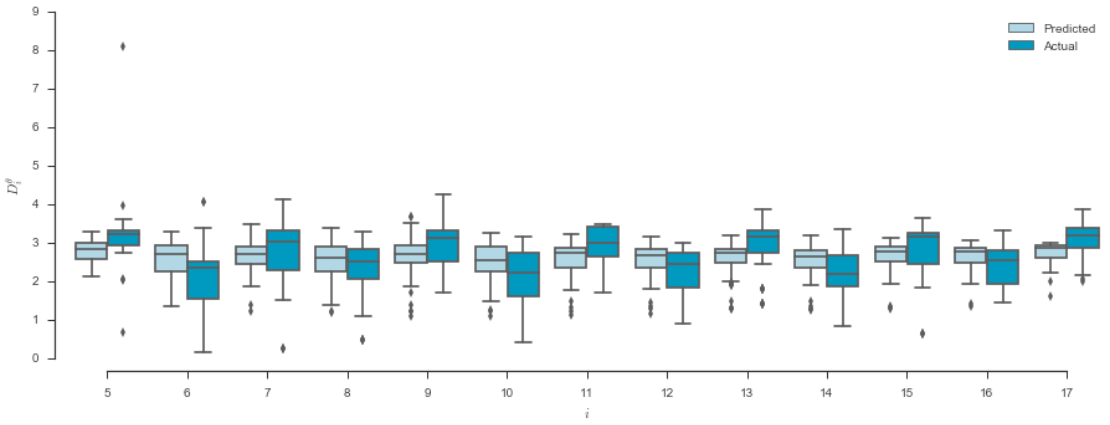

Fig. 4. Comparison between the actual and predicted defect level using LSTM_H with $n = 4$ and $\theta = 60$.

5. Conclusion

SPP is a sensitive process, where many process parameters can influence the quality of the SPP results. In this research, stencil cleaning is considered as a critical factor that can be controlled by applying the RNNs. Based on the history SPP process information, such as printing speed and printing performance, the future process performance can be predicted, which is applied to decide the cleaning cycle. The different configurations of the predictive setting are studied in this research. Results show that different models have different performance on predicting different printing results. Generally, LSTM_S and LSTM_H can be used to enhance the stencil cleaning cycle prediction process.

The next step of this research can be considered from several perspectives. For instance, cleaning cycle test can be conducted based on practical experiment. The LSTM model can be extended to include more layers and more printing process input information.

References

[1] Davies, L., Gather, U., 1993. The identification of multiple outliers. Journal of the American Statistical Association 88, 782–792.
[2] Ho, S., Xie, M., Goh, T., 2002. A comparative study of neural network and box-jenkins arima modeling in time series prediction. Computers & Industrial Engineering 42, 371–375.
[3] Lau, F.K., Yeung, V.W., 1997. A hierarchical evaluation of the solder paste printing process. Journal of Materials Processing Technology 69, 79–89.
[4] Meng, Z., Watanabe, S., Hershey, J.R., Erdogan, H., 2017. Deep long short-term memory adaptive beamforming networks for multichannel robust speech recognition, in: Acoustics, Speech and Signal Processing (ICASSP), 2017 IEEE International Conference on, IEEE. pp. 271–275.
[5] Pan, J., Tonkay, G.L., Storer, R.H., Sallade, R.M., Leandri, D.J., 2004. Critical variables of solder paste stencil printing for micro-bga and fine-pitch qfp. IEEE Transactions on Electronics Packaging Manufacturing 27, 125–132.
[6] Poon, G.K., Williams, D., 1999. Characterization of a solder paste printing process and its optimization. Soldering & surface mount technology 11, 23–26.
[7] Rodriguez, P., Cucurull, G., Gonzàlez, J., Gonfaus, J.M., Nasrollahi, K., Moeslund, T.B., Roca, F.X., 2017. Deep pain: Exploiting long short-term memory networks for facial expression classification. IEEE transactions on cybernetics .
[8] Rutkowska, A., 2015. Properties of the cox–stuart test for trend in application to hydrological series: the simulation study. Communications in Statistics-Simulation and Computation 44, 565–579.